DEVELOPMENT OF HYALURONIC ACID HYDROGELS FOR NEURAL STEM CELL ENGINEERING

A Thesis Submitted to the Temple University Graduate Board

In Partial Fulfillment of the Requirements for the Degree Master of Science in Bioengineering

---

by
Weili Ma
July 2015

Examining Committee Members:
Dr. Won H. Suh, Ph.D., Bioengineering
Dr. Cezary Marcinkiewicz, Ph.D., Bioengineering
Dr. Peter Lelkes, Ph.D., Bioengineering
Dr. Philip Lazarovici, Ph.D., Bioengineering

ABSTRACT

In this work, a hydrogel made from hyaluronic acid is synthesized and utilized to study neural stem cell behavior within a custom tailored three dimensional microenvironment. The physical properties of the hydrogel have been optimized to create an environment conducive for neural stem cell differentiation by mimicking the native brain extracellular matrix (ECM) environment. The physical properties characterized include degree of methacrylation, swelling ratios, enzymatic degradation rates, and viscoelastic moduli. One dimensional proton nuclear magnetic resonance (1HNMR) confirms modification of the hyaluronic acid polymers, and is used to quantify the degree of methacrylation. Rheological measurements are made to quantify the viscoelastic moduli. Further post-processing by lyophilization leads to generation of large voids to facilitate re-swelling and cell infiltration. ReNcell VM (RVM), and adult human neural stem cell line derived from the ventral mesencephalon, are cultured and differentiated inside the hydrogel for up to 2 weeks. Differentiation is characterized by immunocytochemistry (ICC) and real time quantitative polymerase chain reaction (RT-qPCR).

I dedicate this thesis to my parents

for all their sacrifices and support

for me to be where I am today.

ACKNOWLEDGMENTS

I would like to thank Dr. Won H. Suh for providing me with research guidance and funding required for this project, and all the members of the Suh lab for their individual contributions. I thank my thesis committee members Dr. Peter Lelkes, Dr. Cezary Marcinkiewicz, and Dr. Philip Lazarovici for their invaluable feedback and guidance. I also thank Dr. Hong Cheng from Fox Chase Cancer Center for help with HNMR data collection.

TABLE OF CONTENTS

LIST OF FIGURES

LIST OF TABLES

CHAPTER 1: INTRODUCTION

1.1 Background

Over the last few decades, our understanding of cellular behavior and mechanisms has grown tremendously thanks to *in vitro* studies. However, the traditional method of growing cells tissue culture plastic places the cells in an overly simplified microenvironment. Inside the body, cells are surrounded by an extracellular matrix (ECM) which has unique physicochemical properties depending on tissue type[1] (Figure 1). The ECM provides both mechanical and biochemical cues for cells and have been shown to play roles in survival, proliferation, and migration. In addition, it is important to realize that the cell-matrix interaction is bi-directional, and that the cells are also able to affect its microenvironment (i.e. degradation and ECM remodeling). Cell-matrix interactions need to be preserved for development of accurate, *in vitro* culture systems[2,3]

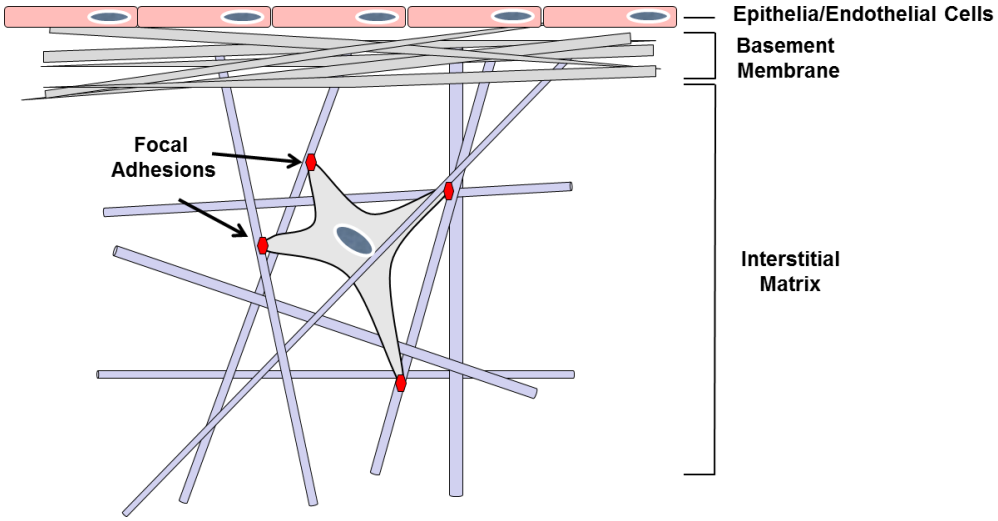

Figure 1. Simplified schematic of the extracellular matrix

Compared to a two dimensional (2D) culture system using a monolayer of cells on tissue culture plastic, a three dimensional (3D) culture system has many new factors

that must be considered. First, suitable biomaterials must be chosen so that the cell-matrix interactions can be well regulated and highly reproducible. This is an important parameter since quality control will be very important for producing consistent matrices. Second, materials with innate bioactivity should be considered for use in 3D cell culture. Although both synthetic and natural biomaterials can be used to make tissue engineering scaffolds, there are advantages to using one type over another. For synthetic materials, the production and processing is easy to control and can provide constructs with highly reproducible properties. However, these materials typically require further modification with cell-recognition ligands in order to interact with cells[4] . Natural biomaterials possess an innate ability to interact with cells, due to their source. However, these biomaterials often have poor structural integrity and require further modification to increase its mechanical stability[5]. Finally, Biomaterials being developed as a tool for cell culture also need to be tailored to specific applications and experiments in which they are to be used[6,7]. Aside from biochemical properties, the physical properties of the hydrogel such as swelling ratios, viscoelasticity, and degradation should also be considered[7]. Many previous studies have shown that stem cell fate can be directed by the mechanical stiffness of the matrix[8-10].

Certain biomaterials can be processed into structures called hydrogels. Hydrogels are a network of hydrophilic, crosslinked polymer chains which imbibe water. Due to its high water content and controlled degradation mechanics, hydrogels have been used frequently in the biomedical field to deliver drugs and encapsulate cells for transplantation[11]. HA-based hydrogels have been heavily investigated over the years due to its innate bioactivity. The chemical structure of HA contains several functional groups

that can be used for crosslinking and conjugation chemistries[12,13]. Its physical properties such as swelling ratio, degradation, and viscoelastic moduli have been shown to be correlated with the degree of modification and crosslinking densities[14]. Fine tuning the control over its physical properties allows it to be used in a variety of soft tissue engineering applications[15].

In order to study the behavior of neural stem cells *in vitro,* a suitable hydrogel system needs to be developed that match the physicochemical properties of native brain tissue as closely as possible. Unlike the ECM found in other parts of the body, the composition of the brain ECM is rather unique (Figure 2).

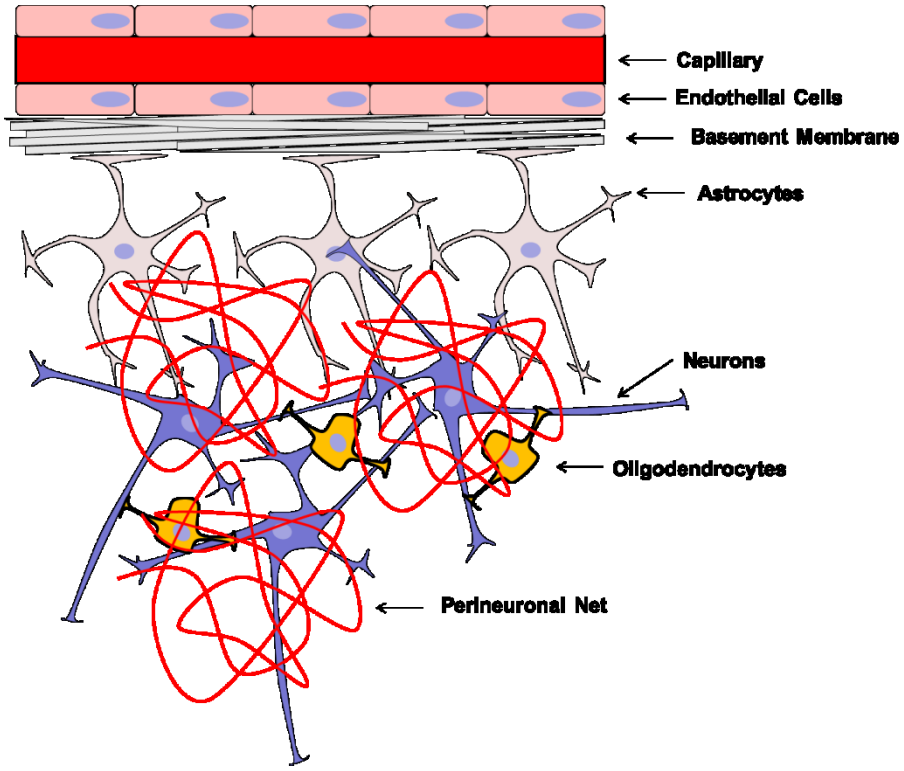

Figure 2. Simplified schematic of brain extracellular matrix

First, there is a highly selective barrier formed by a tight junction of endothelial cells called the blood brain barrier (BBB). The BBB separates the blood from the rest of the brain extracellular space, and only allows entry of small, non-polar molecules and

water. Also, the interactions between the astrocytes and endothelial cells are very important to maintaining the integrity of the BBB[16]. Second, there is a basal lamina which is rich in laminin, but other common proteins such as fibronectin, vitronectin, and collagen are nearly absent. Finally, the interstitial space does not contain and fibrous matrix proteins. Instead, structures called perineuronal nets (PNN) surround the cell bodies[17].

The PNN is a structure which can be broken down into several key components (Figure 3). The backbone of the structure is hyaluronic acid, a naturally occurring polysaccharide. Link proteins, chondroitin sulfate proteoglycans (CSPGs) of the lectican family, and tenascin-R are also found throughout the structure. The formation of the PNN has been correlated with maturation of neural tissue. Furthermore, it has been correlated with loss of neural plasticity. However, it has been reported that enzymatic removal of the CSPGs results in enhanced plasticity and axon regeneration capabilities[18,19].

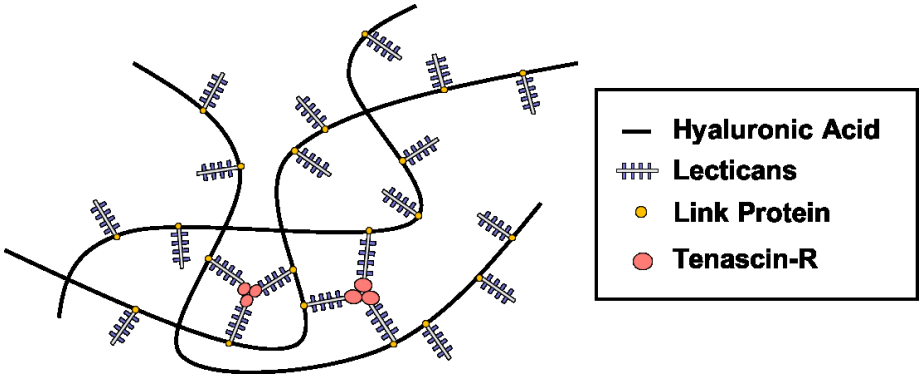

Figure 3. Major components of the perineuronal net

Hyaluronic acid (HA) is a naturally occurring polysaccharide that is found throughout the body. HA has been utilized frequently to fabricate hydrogels for tissue engineering[12,20,21]. It is commonly found the synovial joints, but is also abundant in the brain extracellular space. HA in its monomeric form is a disaccharide consisting of D-

glucuronic acid and *N*-acetylglucosamine, joined together by 1,3 and 1,4 glycosidic bonds (Figure 4). HA polymers are naturally degraded inside the body by hyaluronidase enzymes. The enzyme has also been used by many groups for degradation studies on crosslinked HA hydrogels[20,21].

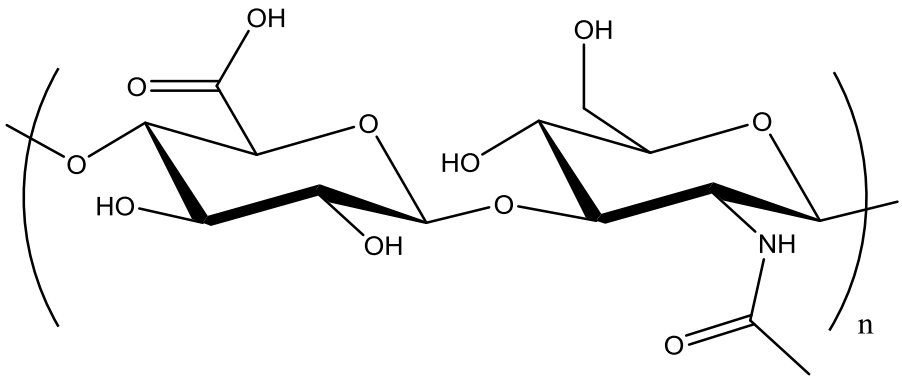

Figure 4. Chemical structure of hyaluronic acid

For the work described in this thesis, in order to recreate an accurate model of the brain ECM *in vitro*, HA has been chosen as the starting material. In order to increase the structural integrity, crosslinks will be introduced to create bonds between individual polymer chains. Several methods have been described for crosslinking of HA polymers[22,23]. For this project, a radical polymerization method will be used due to its cleanliness in reaction by-products compared to chemical methods. Furthermore, due to the nature of radical polymerization, crosslinking will occur more rapidly and gelation time will be quicker and more controlled[24,25]. In order to generate an HA polymer that can be radically polymerized, methacrylate moieties will be chemically conjugated to the *N*-acetylglucosamine subunits at the 6-hydroxyl position by ester bond (Figure 5).

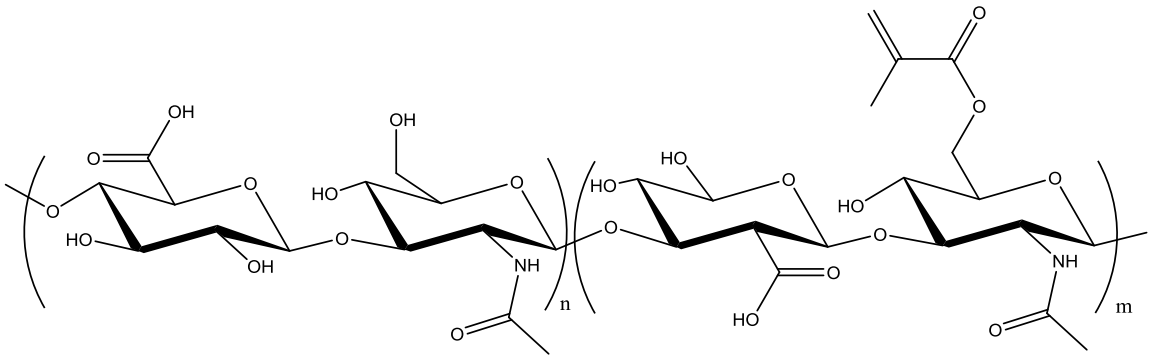

Figure 5. Methacrylated hyaluronic acid structure consisting of modified and unmodified subunits

1.2 Significance and Need

In the central nervous system (CNS), there are several diseases which currently have no cure. One of the most widely studied is the neurodegenerative diseases, such as Alzheimer's Disease (AD) and Parkinson's Disease (PD). Although the mechanisms behind neurodegenerative diseases such as AD and PD are quite different, the result is a loss of neural function over time. This can be caused by both loss of synaptic connections between the neurons or apoptosis of neural cells. In any case, unlike many other cell types in the body neurons are incapable of self-regeneration and mitosis. Instead, neural functions can only be recovered by replacement of damaged neurons by healthy neurons through stem cell differentiation or cell therapy[26,27].

In the recent years, stem cell therapies for treatment of neurodegenerative diseases have become an interesting topic in the field of personalized medicine. Many types of stem cells, including embryonic[28], mesenchymal[29], neural[9,10], and induced pluripotent stem cells[30], have been successfully differentiated into neural cell types. One of the major areas of research in neural stem cell differentiation is controlled differentiation into specific cell types by modulating different factors (Table 1). Identification of key

signaling components will be crucial for efficiently directing differentiation of stem cells into desired cell types for transplantation.

Factors for Directed Differentiation of Neural Stem Cells	
Soluble Factors	Brain Derived Neutrophic Factor (BDNF)[31,32] Nerve Growth Factor (NGF)[33,34] Retinoic Acid (RA)[35,36] Lithium Chloride (LiCl)[37,38]
Matrix Properties	Substrate Stiffness[9,10,39,40]
Other	Electrical Stimulation[41-43]

Table 1. Factors involved in the directed differentiation of neural stem cells

Most of the factors related to neural stem cell differentiation were discovered using traditional *in vitro* culture methods on tissue culture plastics. In neural development, there is both spatial and temporal regulation of a variety of signaling pathways and factors which determines the overall outcome of the stem cells. For a long time, it has been reported that basic fibroblast growth factor (bFGF) only affected the proliferation and not differentiation of neural stem cells. However, when bFGF is introduced to neural stem cells in a 3D culture system, it played roles in both proliferation and differentiation[44]. There are still many unknown factors regarding neural stem cell differentiation, especially when transitioning into the use of 3D *in vitro* culture systems. In order to increase our understanding of neural stem cell differentiation and behavior, an accurate but simple 3D model of the brain ECM needs to be developed.

CHAPTER 2: GOALS AND AIMS

In this study, a photopolymerizable hyaluronic acid hydrogel is synthesized to create a structural mimic of the native brain ECM for neural stem cell differentiation. An optimized 3D culture system will allow for modeling of stem cell behavior and growth in a microenvironment that better mimic *in vivo* conditions compared to tissue culture plastic. The mechanical properties of the HA hydrogel will be matched with those of adult human brain tissue. There are many factors which can affect the modulus of brain tissue, including disease, age, species, and gender. A technique called magnetic resonance elastography has been recently used to determine the modulus of live, adult human brain tissue which has been reported to be 2.7 kPa and 3.1 kPa for white and grey matter, respectively[45].

By modulating the amount of reactants during synthesis of the hydrogels, HA with different degrees of modification (DM) will be synthesized and the DM will be quantified by ^{1}HNMR. Commonly used cell adhesion coating proteins such as laminin, collagen, and gelatin will be used to further enhance cellular interactions with the hydrogel. The mRNA of differentiated neural stem cells (NSCs) will be collected at 1 and 2 week time points for real time quantitative polymerase chain reaction (RT-qPCR). Gene expression levels of neural stem cell markers SOX2 and Nestin, neural lineage markers β3-tubulin and MAP2, astrocyte marker GFPA, and oligodendrocyte marker OMG will be analyzed. Immunocytochemistry staining for neural stem cell marker nestin and neural lineage marker β3-tubulin will be observed under fluorescent confocal microscopy.

In order to achieve this goal, the following specific aims are utilized:

1) Synthesis of methacrylated hyaluronic acid polymers with varying degrees of methacrylation
2) Characterization of the hyaluronic acid hydrogels and incorporation of cell matrix proteins to promote enhanced bioactivity
3) Neural stem cell differentiation study using an HA hydrogel optimized to simulate brain ECM

The methacrylated hyaluronic acid (MeHA) polymers will need to have their degrees of modification determined by ^{1}HNMR. Depending on the synthesis conditions, such as amount of reactants used, MeHA with low, medium, and high degrees of modification will be synthesized to test their effects on the viscoelastic moduli of the crosslinked hydrogels will be analyzed by oscillatory rheology testing using a frequency sweep. The effects of total energy input required to initiate the crosslinking will also be analyzed.

Although photo-initiators do not generate any toxic chemical by-products, its activated form can be highly cytotoxic to certain cell types[46]. Furthermore, the prolonged exposure to high intensity light may cause harm to the cells. It is expected that most cells will die due to light exposure and cytotoxicity of the photoinitiator. Alternatively, the hydrogel formation and cell seeding process should be separated. Lyophilization is a method often used to fabricate tissue engineering scaffolds. This leaves large voids that can facilitate re-swelling and cellular infiltration. The mechanical strength of the hydrogel structure will need to be re-evaluated following lyophilization.

Once a desired modulus range is reached, cell matrix proteins laminin, type 1 collagen, and gelatin will be incorporated into the hydrogels separately to try and enhance its bioactivity. These proteins are often used as coating materials to promote cellular adhesion to biomaterials and tissue culture plastic. A concentration of 20 μg/mL will be utilized, in order to match the average coating density used in 2D culture.

ReNcell VM (RVM), an adult human neural stem cell line derived from the ventral mesencephalon, will be differentiated in the MeHA hydrogels and genetic expression of various neural stem cell and neural lineage markers will be analyzed. Comparisons will be made against RVM grown on laminin coated tissue culture plastic. Cells will be stained for neural stem cell marker nestin and neural lineage marker β3-tubulin for immunocytochemistry (ICC) and fluorescence microscopy analysis. The relative percentages of protein expression will be quantified by cell counting. To retrieve the mRNA from encapsulated cells, the hydrogel will first be degraded using the hyaluronidase enzyme[13]. The RT-qPCR data will be compared against the ICC images to obtain a full set of differentiation data.

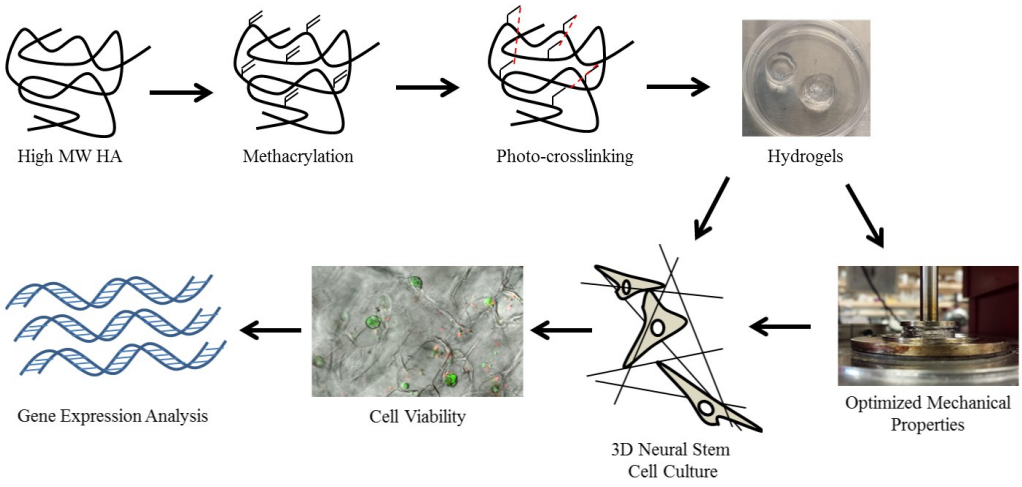

Figure 6. Project overview

CHAPTER 3: MATERIALS AND METHODS

Synthesis of Methacrylated Hyaluronic Acid (MeHA)

1.5 MDa sodium hyaluronate (Lifecore HA15M) was dissolved in nanopure water at a concentration of 10 mg/mL. The solution was chilled on ice for 5 minutes and the pH was adjusted to be between 8 to 10 by dropwise addition of 5 M sodium hydroxide (NaOH). While stirring on ice, various molar excess of methacrylic anhydride (MA) was added dropwise to the solution. The molar excess was calculated with respect to the primary alcohol on the *N*-acetylglucosamine subunit of HA. During this step, the pH was monitored and kept between 8 to 10 by addition of 5 M NaOH when necessary. After addition of MA, the solution was allowed to continue stirring in the dark at 4^{o}C for 24 hours. The MeHA solution was then dialyzed against nanopure water for 72 hours, changing the water daily. The dry product was obtained by lyophilization at 20 mbar and -58^{o}C.

Degree of Methacrylation (DM)

The MeHA samples were dissolved at 10 mg/mL in deuterium oxide and analyzed using ^{1}HNMR (Bruker Ultra-Shield 600 MHz). DM was calculated by taking the ratio of integrals of the methacrylate protons at 2, 5.8, and 6.2 ppm with respect to the peak at 1.9 ppm for the methyl proton of the *N*-acetylglucosamine subunit.

Hydrogel Preparation

Dry MeHA polymers were cut into pieces and sterilized by UV irradiation for 30 minutes inside a biosafety cabinet. A 0.05% wt/v photoinitiator solution (Irgacure 2959) was prepared by dissolving the photoinitiator in nanopure water. The photoinitiator

solution was filter sterilized through a 0.22 μm membrane. The MeHA polymers were then dissolved in the photoinitiator solution at 10 mg/mL, and allowed to stir overnight in the dark at room temperature to completely dissolve. The precursor solution was crosslinked using a metal halide light source (EXFO X-Cite 120Q PC). The power density can be controlled by changing the distance between the light source and the sample. In the initial experiments a power density of 10 mW/cm^2 was used. By modulating the exposure time, a total energy input ranging from 0.3 to 0.9 J/cm^2 was used to crosslink the hydrogels for experiments.

Rheology

Hydrogel disks (n = 3 per group) were prepared by pipetting the precursor solution of MeHA with varying DM between two glass slides with a 1 mm spacer.

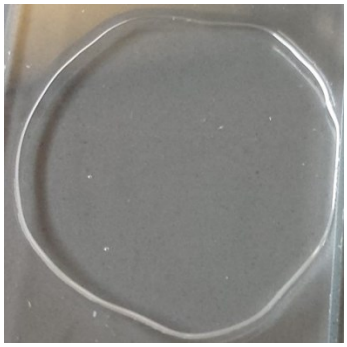

Figure 7. 1 mm thick photo-crosslinked MeHA hydrogel disks for rheology

An oscillatory frequency sweep was conducted using an ATS Rheosystems STRESSTECH rheometer fitted with a parallel plate measuring system. After pre-loading the hydrogels to a 1 mm gap height, the test platform was heated to 37^{o}C. Excess hydrogel was trimmed from the measuring plate before starting the test. The storage (G') and loss (G") moduli were evaluated by an oscillatory frequency sweep ranging from 0.1

to 10 Hz at 0.1% strain. Moduli between sample sets were compared using the G' and G" values at 1 Hz.

Incorporation of Cell Adhesion Proteins

After determining the optimal formulation to yield a hydrogel with similar storage modulus as adult human brain, commonly used cell adhesion proteins were incorporated into the precursor solution. Immediately before crosslinking, laminin (Sigma L2020), rat tail collagen type I (BD Biosciences 354236), or bovine gelatin (Sigma-Aldrich G9382) were mixed into the precursor solution at 20 μg/mL.

Swelling and Degradation

The swelling ratios of the hydrogels with and without cell matrix proteins (n = 3 per group) in PBS were tested by monitoring the weight change over time. 200 μL droplets of hydrogel precursors were crosslinked in 35 x 10 mm petri dishes and the hydrogels were lyophilized for 24 hours and weighed to obtain the dry weight (W_D). The hydrogels were swollen in PBS for up to 7 days and the wet weight was measured on day 7 (W_S). Before weighing the hydrogels, excess PBS is removed by pipetting and the remaining moisture is removed by gentle tapping with a Kimwipe. The volumetric swelling ratio (Q) was then calculated by the following equation:

$$Q = \frac{W_S - W_D}{W_D}$$

The enzymatic degradation rates of swollen hydrogels were tested by addition of 100 U/mL of bovine hyaluronidase in PBS. After addition of hyaluronidase, hydrogels were placed into an incubator at 37°C and the weight change was monitored over time. After removing the hyaluronidase solution to measure the weights of the hydrogels, the same

hyaluronidase solution was added back into the hydrogels instead of fresh hyaluronidase solutions.

Neural Stem Cell Maintenance

ReNcell VM (RVM), adult neural stem cells derived from the ventral mesencephalon, were maintained in neurosphere form until use. The RVM neurospheres were cultured in T-75 flasks without laminin in serum free neural stem cell maintenance medium containing 20 ng/mL epidermal growth factor (EGF) and 20 ng/mL basic fibroblast growth factor (bFGF). Prior to seeding in lyophilized hydrogels, the neurospheres were dissociated using Accutase and transferred to T-75 flasks coated with laminin for rapid expansion.

Neural Stem Cell Seeding and Differentiation

RVM was recovered from laminin coated T-75 flasks by treatment with Accutase and gentle shaking. 48-well plates containing lyophilized hydrogels were pre-warmed to 37^{o}C and 2D plates were coated for at least 4 hours with 20 µg/mL laminin (Sigma L2020). RVM was seeded at 1 x 10^5 cells per well and allowed to proliferate in serum free maintenance medium containing 20 ng/mL EGF and bFGF overnight in the incubator. Differentiation for RVM was initiated by withdrawal of growth factors from the culture medium. Differentiation was maintained for 2 weeks and medium was refreshed every 48 hours. Since not all the medium can be removed from hydrogels by pipetting, a 2D control simulating conditioned medium is also used. In these wells, only half the medium was exchanged every 48 hours.

Immunocytochemistry

Excess medium was removed from the 8-well plates and the samples were rinsed with PBS three times with gentle shaking. 4% paraformaldehyde (PFA) was added for 15 minutes to fix the samples. After removal of PFA, the hydrogels were rinsed again with PBS three times. A solution containing 0.3% Triton-X and 3% Donkey serum in PBS was added for 30 minutes for blocking and permeation. The samples were then rinsed again with PBS three times and primary antibodies (Nestin and β3-Tubulin) were added at a 1:100 dilution at 4^{o}C overnight. Primary antibodies were removed and the samples were rinsed with PBS three times with gentle shaking, and secondary antibodies (Alexa Fluor 488 for Nestin and 555 for β3-Tubulin) were added for 2 hours at 1:200 dilutions in the dark at room temperature. After removing secondary antibodies, the samples were rinsed with PBS three times. Nuclei were stained with DAPI for 10 minutes and rinsed with PBS. The cells were stored at 4^{o}C in PBS until microscopy analysis. ICC samples were imaged using a confocal fluorescent microscope (Olympus IX-83, EXFO X-Cite 120 PC Lamps). The percentage of cells expressing either nestin or β3-tubulin were determined by cell-counting (n = 3 sections of a well per group).

Quantitative Reverse Transcript Polymerase Chain Reaction (RT-qPCR)

One day prior to differentiation end time points (1 and 2 weeks), differentiation medium was changed to differentiation medium containing 100 U/mL hyaluronidase. Degraded HA, medium, and cells were combined from same experimental group wells (n = 6 per plate, theoretically 6 x 10^5 cells) and transferred to 15 mL conical tubes. Cell

pellets were separated by centrifugation at 2000 RPM for 5 minutes. After removal of medium and degraded HA, cell lysate was added to the conical tubes. The mRNA was isolated and purified using an Ambion mirVana kit. The concentration and purities of mRNA were analyzed using a plate reader (Tecan Infinite 200 Pro). Samples with concentrations of mRNA samples were below 20 ng/μL were placed in a vacuum concentrator for 30 minutes.

The concentrations of mRNA were normalized to the lowest concentration within the sample set before cDNA synthesis with a high capacity kit from Applied Biosystems using random primers. This was to ensure that equal amounts of cDNA are synthesized from the samples. After synthesis of cDNA by reverse transcriptase, real time quantitative PCR is performed using a Taqman assay kit from Applied Biosciences. Genes of interest included internal standards GAPDH and β-Actin, neural stem cell markers SOX2 and Nestin, neural marker β3-tubulin, mature neural marker MAP2, astrocyte marker GFAP, and oligodendrocyte marker OMG. The cDNA was run for 40 cycles and the cycle threshold values were analyzed.

Statistical Analysis

All statistical analyses were done using the JMP 10 Pro software. Data points were inputted into JMP data tables and a distribution was calculated using the Fit Y by X function. Significance between groups was analyzed with alpha values of 0.05 and 0.01. Mean comparisons were performed using ANOVA and Tukey's HSD.

CHAPTER 4: RESULTS AND DISCUSSION

^{1}HNMR was used to quantify the degree of methacrylation (DM). Synthesis of methacrylated hyaluronic acid (MeHA) was successful as determined by the methacrylate proton peaks in the ^{1}HNMR spectrum. The control spectrum is from unmodified hyaluronic acid (HA) dissolved in deuterium at 10 mg/mL (Figure 8A). After modification, methacrylate proton peaks can be seen at 1.9, 5.8, and 6.2 ppm (Figure 8B). DM is calculated by the ratio of the sum of these peaks to the methyl proton peak at 2.1 ppm.

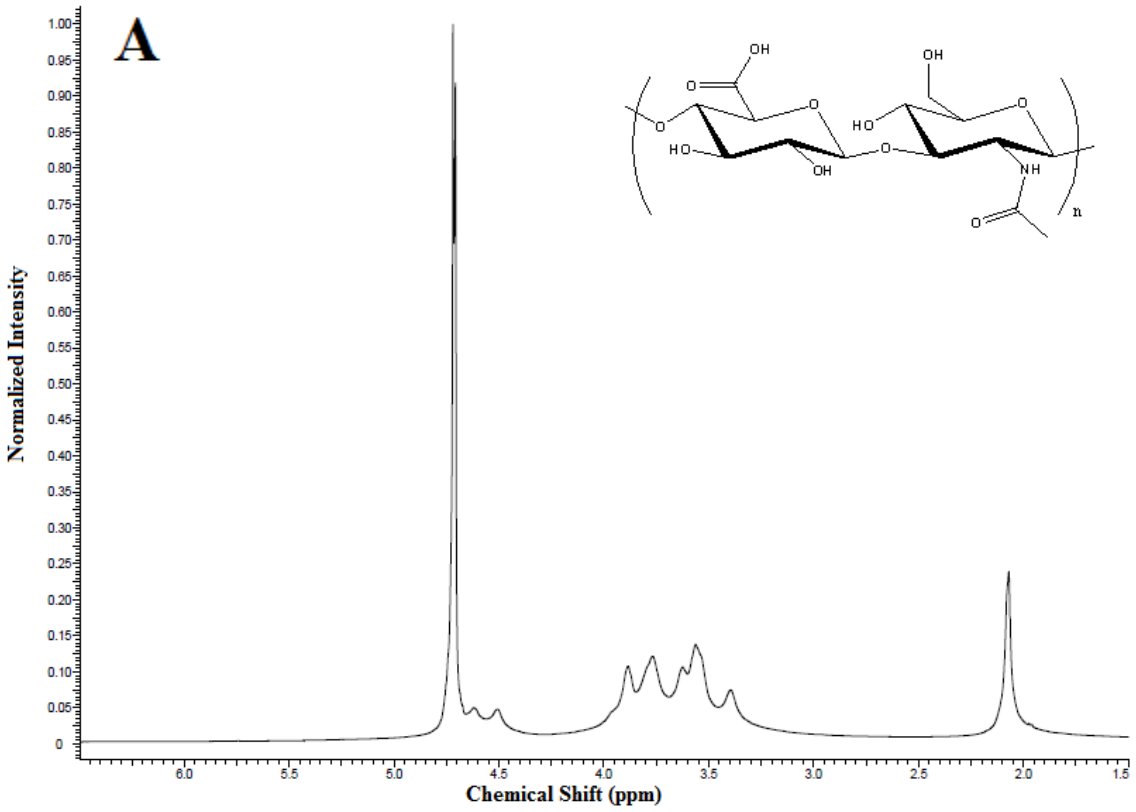

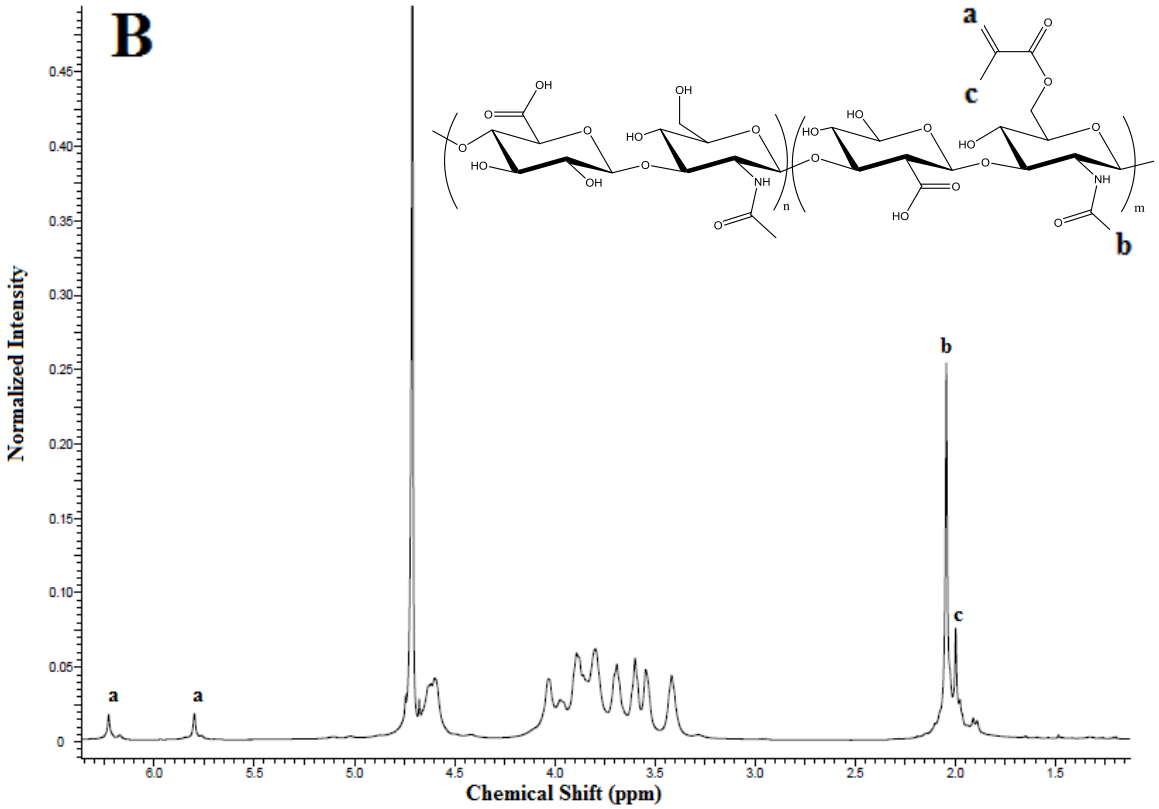

Figure 8. [1]HNMR of HA (A) and MeHA (B) dissolved in deuterium

The degree of methacrylation (DM) could be controlled by modulating the amount of reactant used in the synthesis reaction. The calculated DM values of MeHA made from 5, 10, and 20 molar excess of methacrylic anhydride (MA) were 58±0.02%, 74.33±0.01%, and 94±0.05%, respectively.

An oscillatory frequency sweep with controlled strain at 0.1% was performed to determine the storage and loss moduli of the hydrogels. All samples were loaded to 1 mm gap height and preheated to 37°C prior to testing. Using a parallel plate system, a frequency sweep between 0.1 to 10 Hz was performed at 0.1% strain to measure the response. By modulating the degree of methacrylation, hydrogels could be formed with a storage modulus ranging from 0.4 to 1 kPa (Figure 9).

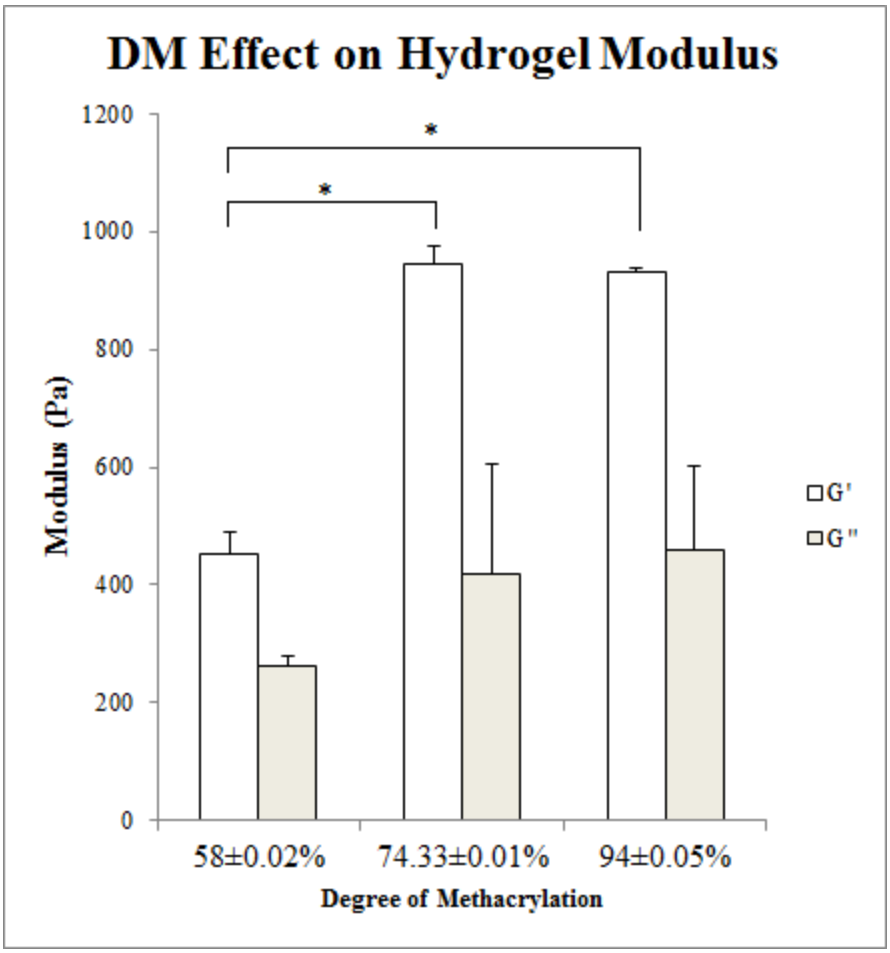

Figure 9. Measured storage (G') and loss (G") moduli from crosslinked MeHA hydrogels under oscillatory frequency sweep.

As expected, the lowest DM hydrogels had a lower viscoelastic modulus compared to the other samples. However, there was no significant difference between samples with DM of 74.33±0.01% and 94±0.05%.

For photo-polymerization, the total energy input can affect the degree of crosslinking, and consequently the viscoelastic moduli. The effect of total energy input on viscoelastic modulus was tested using hydrogels with DM 58±0.02% (Figure 10). In these results, the hydrogel precursors were exposed to a 10 mW/cm^2 light source for 30, 60, and 90 seconds.

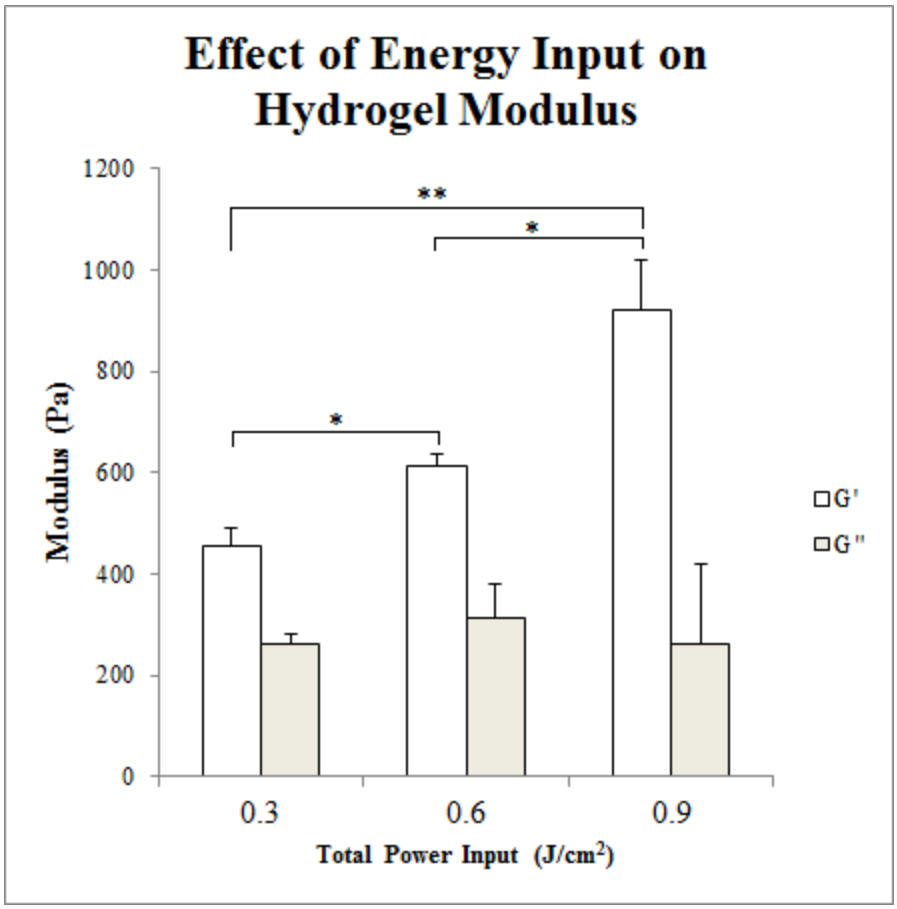

Figure 10. Measured G' and G" values at 1 Hz for hydrogels with DM 54±0.02% crosslinked with varying amounts of energy input.

As expected, the storage modulus increases with increased energy input. This is likely an effect due to the photoinitiator being used (Irgacure 2959). It has been shown that Irgacure 2959 has a max absorbance around 280 nm, but can still be effectively activated by longer wavelengths given enough energy input[47]. Unfortunately, wavelengths in the deep UV range (UVC and UVB) are mutagenic to most cell types and cannot be used for encapsulation[48]. An alternative method that may warrant an investigation for future studies involves the use of visible light photoinitiators, which can activate more efficiently using longer wavelength light sources.

Direct hydrogel encapsulation of ReNcell VM (RVM) adult neural stem cells were tested to see whether or not there were cytotoxic effects from the activated photoinitiator and the light source. After forming a cell pellet, the cells were homogenously mixed into a hydrogel precursor solution containing 0.05% photoinitiator. The precursor solution containing cells were aliquoted into 24-well plates (n = 3) at 200 µL per well, and each hydrogel contained roughly 1 x 10^5 cells. Another group (n = 3) of RVM were seeded on laminin coated surfaces at 1 x 10^5 cells per well. This group was subjected only to light exposure without any photoinitiator. The cells were exposed to 0.3 J/cm^2 energy input. The cell viability was analyzed with PrestoBlue (Figure 11).

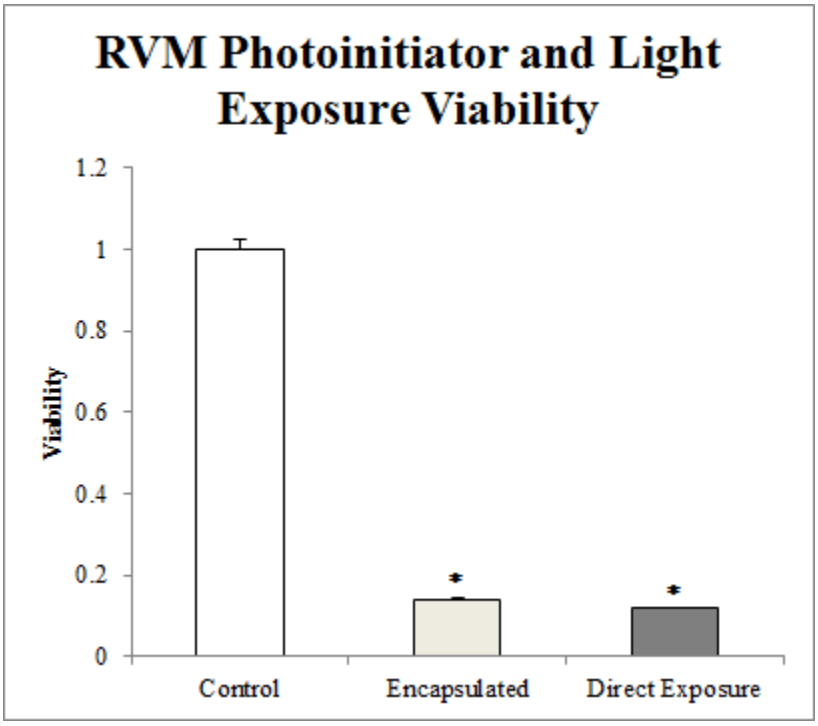

Figure 11. Cytotoxicity of photoinitiator and light exposure on RVM measured by PrestoBlue.

Direct cell encapsulation resulted in low cell viability. This suggests that direct exposure of RVM to the amount of light required for crosslinking is highly cytotoxic. This may be due to the light source being used (EXFO X-Cite 120Q). This light source is designed for

fluorescence microscopy and is not filtered for specific wavelengths. Therefore, there is a spectrum of peak wavelengths being emitted. In the future, a broadband filter may be needed to attenuate the photo-toxicity effects.

Based on the cell viability results, hydrogels needed to be further processed by lyophilization. This would allow for crosslinking and cell seeding to be separated into two steps. Because a hydrogel is mostly comprised of water, the lyophilized hydrogels were allowed to swell for 48 hours in PBS prior to rheology. The effect of lyophilization and re-swelling on the viscoelastic moduli was investigated using hydrogels with DM 54±0.02% with a total energy input of 0.3 J/cm^2 (Figure 12).

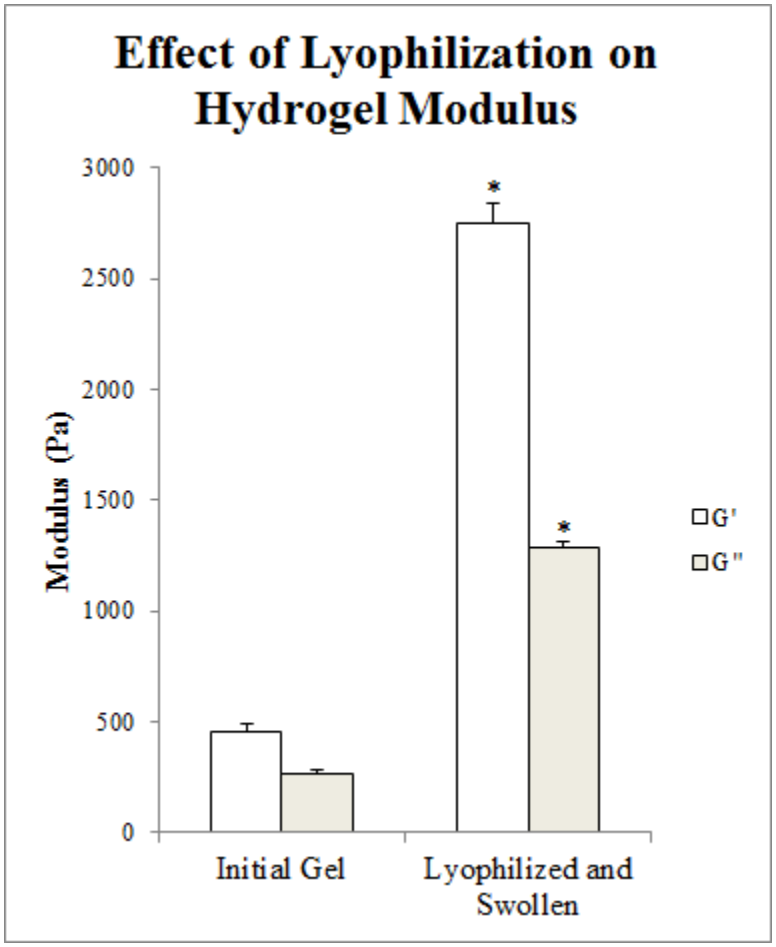

Figure 12. Effect of lyophilization and re-swelling of MeHA hydrogels on the storage (G') and loss (G") moduli.

Post processing by lyophilization and re-swelling in PBS affected its viscoelastic moduli. There was a five-fold increase in both the storage and loss modulus of the hydrogels. These new values closely resemble those which have been reported for adult human brain tissue. Reported values for the storage moduli range of live adult human brain tissue ranges between 2.7 kPa to 3.1 kPa for white and grey matter, respectively[45]. Only lyophilized hydrogels with DM 54±0.02% crosslinked with 0.3 J/cm^2 were used for further experiments

Lyophilization also has some effects on the microstructure of the hydrogel, such as introduction of large voids. It is a technique widely used in tissue engineering to create porous scaffolds. Optical microscopy images of lyophilized hydrogels in 48-well plates were taken to observe these pores. Further analysis will need to be performed to determine how to control pore size efficiently. Scanning electron microscopy will be needed in the future to determine pore size. 2 x 10^5 RVM were seeded into the hydrogels for a preliminary biocompatibility experiment (Figure 13).

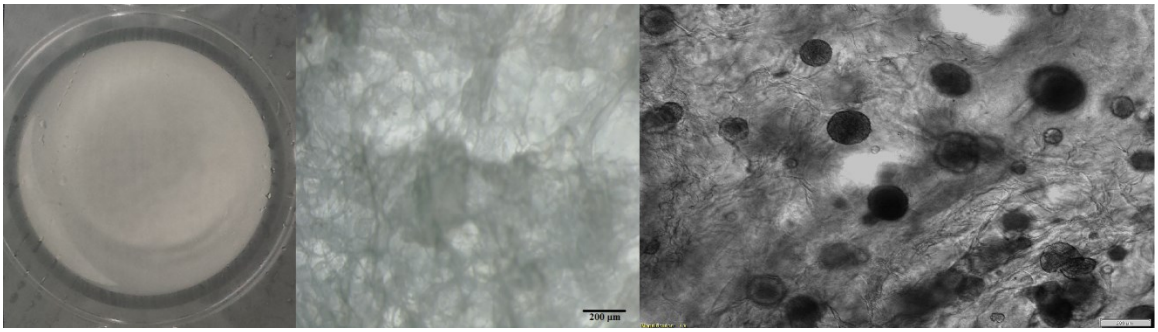

Figure 13. Images of lyophilized MeHA prior to re-welling inside a 48 well plate (left) and a 10x magnification showing macropores (middle). Neural stem cells form neurospheres in the hydrogels after seeding and re-swelling (Right). Scale bar is 200 µm.

A 1 mm hydrogel was formed by crosslinking 100 µL of hydrogel precursor solution in 48-well plates. The lyophilized hydrogels contained large macropores which were sufficiently large enough for cell infiltration, as indicated by optical microscopy

images of the lyophilized hydrogels. RVM seeded into the lyophilized scaffolds formed neurospheres within 24 hours in serum free proliferation medium containing 20 ng/mL epidermal growth factor (EGF) and 20 ng/mL basic fibroblast growth factor (bFGF).

Aside from optimizing the hydrogel's mechanical properties, its bioactive properties were also enhanced. Hyaluronic acid is a ligand for the cell receptors CD-44 and RHAMM, which can be found in certain cell types. In the nervous system, these two receptors and their interactions with HA have been well characterized[49]. However, to improve cellular adhesion and proliferation, cell matrix proteins are often incorporated. For 2D culture, laminin, collagen, and gelatin are the most widely used matrix proteins for coating surfaces. In order to mimic this in a 3D system, the cell adhesion proteins were incorporated into the precursor solution prior to the crosslinking step at 20 μg/mL to try and enhance the bioactivity of the hydrogels.

The swelling ratio of MeHA hydrogels with and without various cell adhesion proteins were calculated by measuring its wet and dry weights. All hydrogels (n = 3 per group) were formed by pipetting 200 μL of the precursor into a 35 x 10 mm petri dish to form a droplet. The concentration of MeHA was kept constant at 10 mg/mL while cell adhesion proteins were diluted to a final concentration of 20 μg/mL. After formation of 58% DM MeHA hydrogels using and energy input of 0.3 J/cm^2, the samples were lyophilized for 24 hours at 20 mbar and -58^{o}C. The dry weights of the hydrogels are then measured. After swelling for 7 days in PBS, the wet weights of the hydrogels are measured (Figure 14). The volumetric swelling ratio is calculated from the wet and dry weights (n = 3 per group).

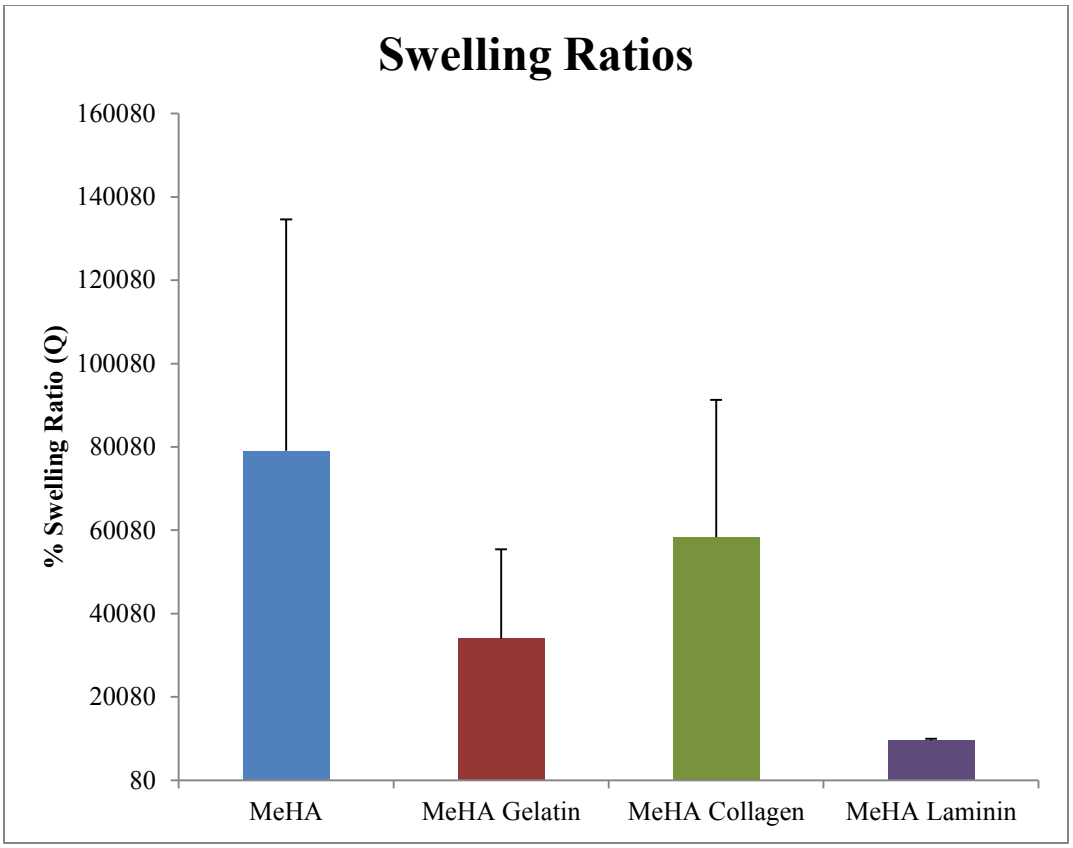

Figure 14. Swelling ratios of MeHA hydrogels with and without additional cell adhesion proteins.

No significant differences were seen between the groups. The swelling rate profile suggests that the hydrogels with and without matrix proteins reach 75 to 100% of its maximum swelling ratio within 24 hours (Figure 15). This also indicates that the 5 fold increase in the modulus after lyophilization is not due to the hydration of the hydrogels. After 48 hours in PBS, the hydrogels should be sufficiently hydrated. Instead, the change in modulus is most likely due to another factor, such as physical entanglement of the polymers during lyophilization or strengthening of mechanical properties due to change in polymer network density.

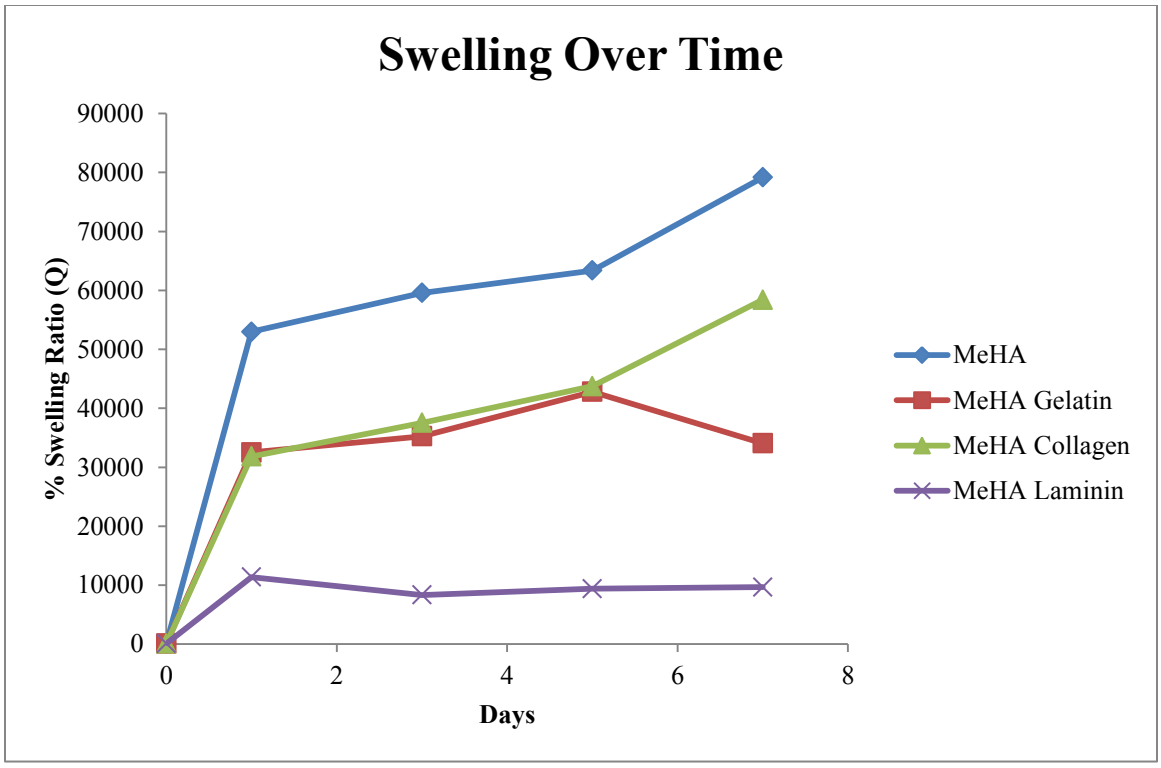

Figure 15. Profile of change in weight of MeHA hydrogels over 7 days in PBS

An enzymatic degradation experiment was performed to determine the degradation rate of the MeHA hydrogels with and without cell matrix proteins. For degradation, PBS containing 100 U/mL bovine hyaluronidase was added to the hydrogels swollen in PBS for 1 week in the swelling ratio experiments. After addition of hyaluronidase, hydrogels were warmed to 37^{o}C in an incubator. Hydrogel degradation was monitored over time by measuring its weight at various time points (Figure 16).

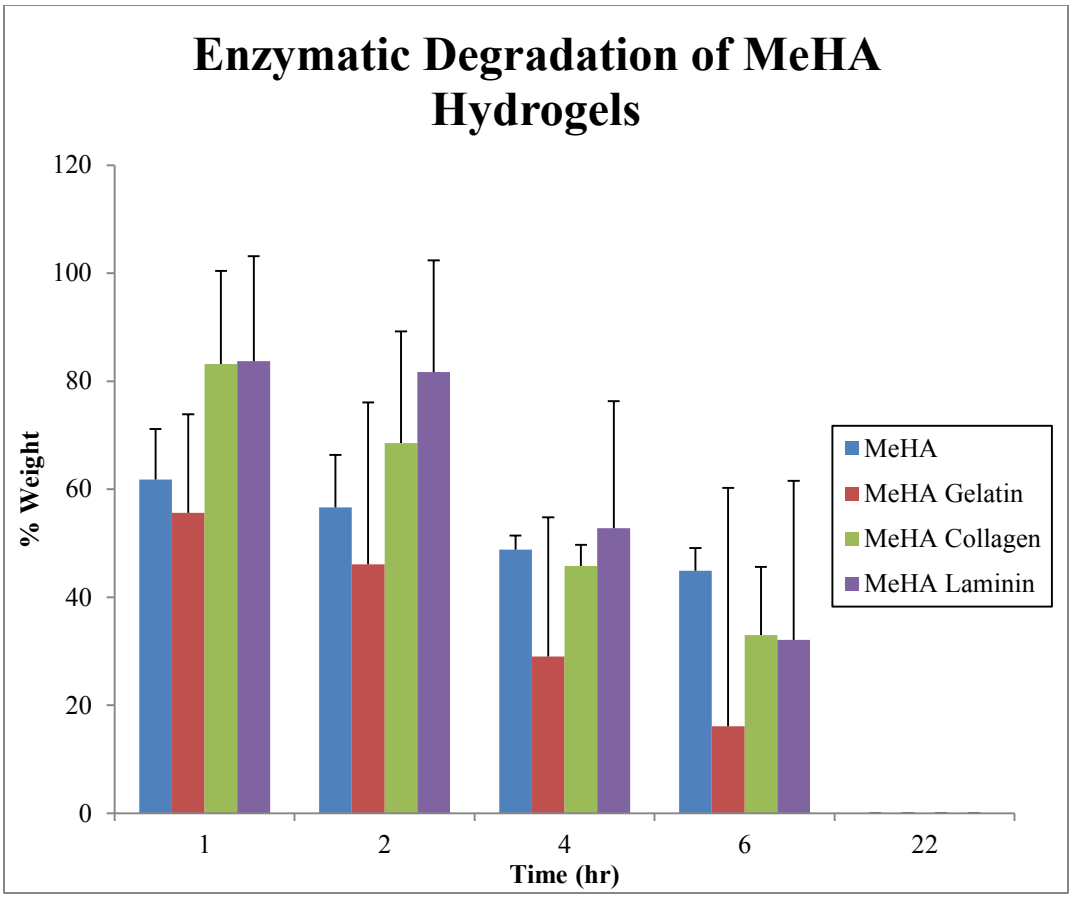

Figure 16. Enzymatic degradation of MeHA hydrogels by bovine hyaluronidase

No significant differences were found between the groups for the degradation rates. All hydrogels were completely degraded after an overnight treatment with 100 U/mL hyaluronidase.

For the RVM differentiation experiments, differentiation was monitored by immunocytochemistry (ICC) and real time quantitative polymerase chain reaction (RT-qPCR) at 1 and 2 week time points. Cells for ICC were seeded in 8-well chambers with laminin coating (2D, Figure 17) or with lyophilized hydrogels (3D, Figure 18 and 19) and stained for the neural stem cell marker nestin and the neural lineage marker β3-tubulin at differentiation end points.

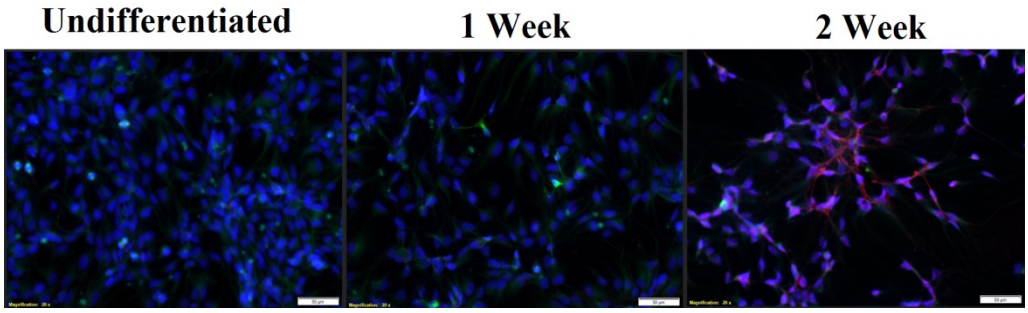

Figure 17. 20x fluorescent microscopy images of RVM on laminin (2D culture).

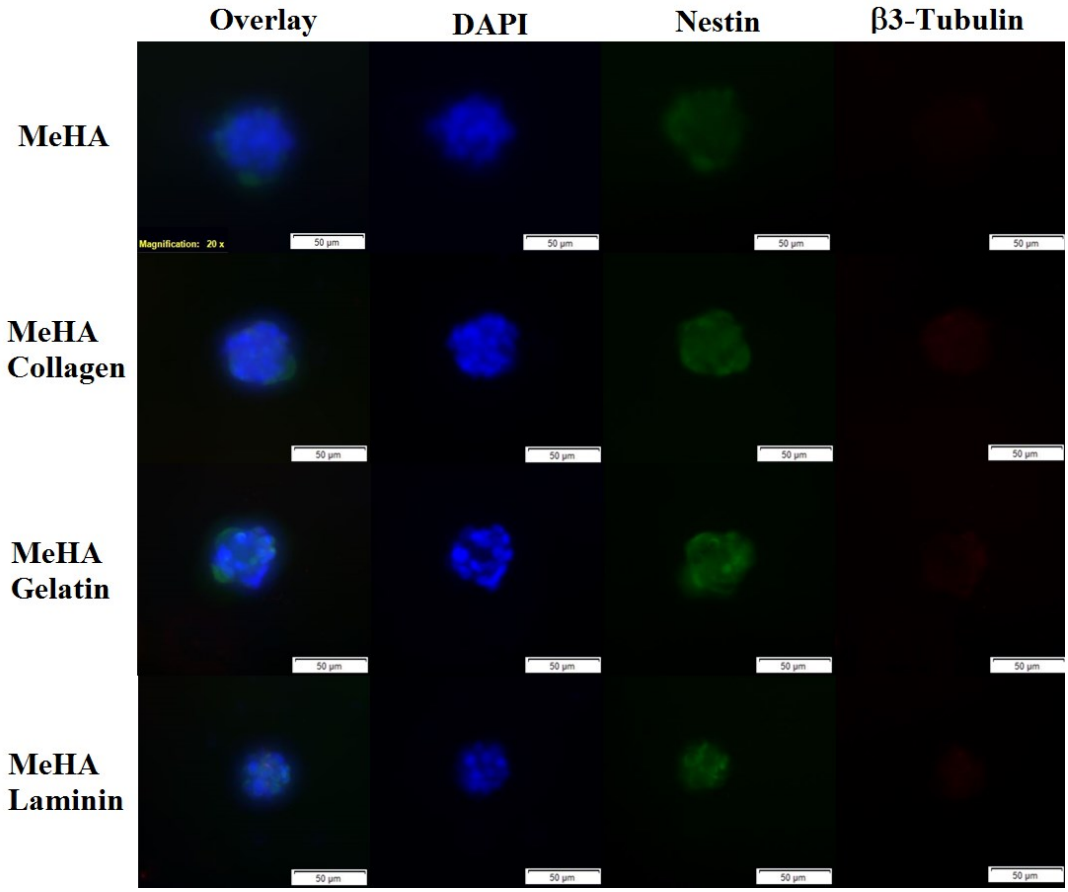

Figure 18. 20x fluorescent microscopy images of RVM encapsulated within hydrogels after 1 week of differentiation.

In both 2D and 3D samples, nestin could be seen after 1 week of differentiation. Almost no β3-tubulin could be seen in the 3D samples, but a small population of cells in the 2D samples stained positively. At 2 weeks of differentiation, the intensity from β3-tubulin increased in both samples, but was more noticeable in the 2D samples.

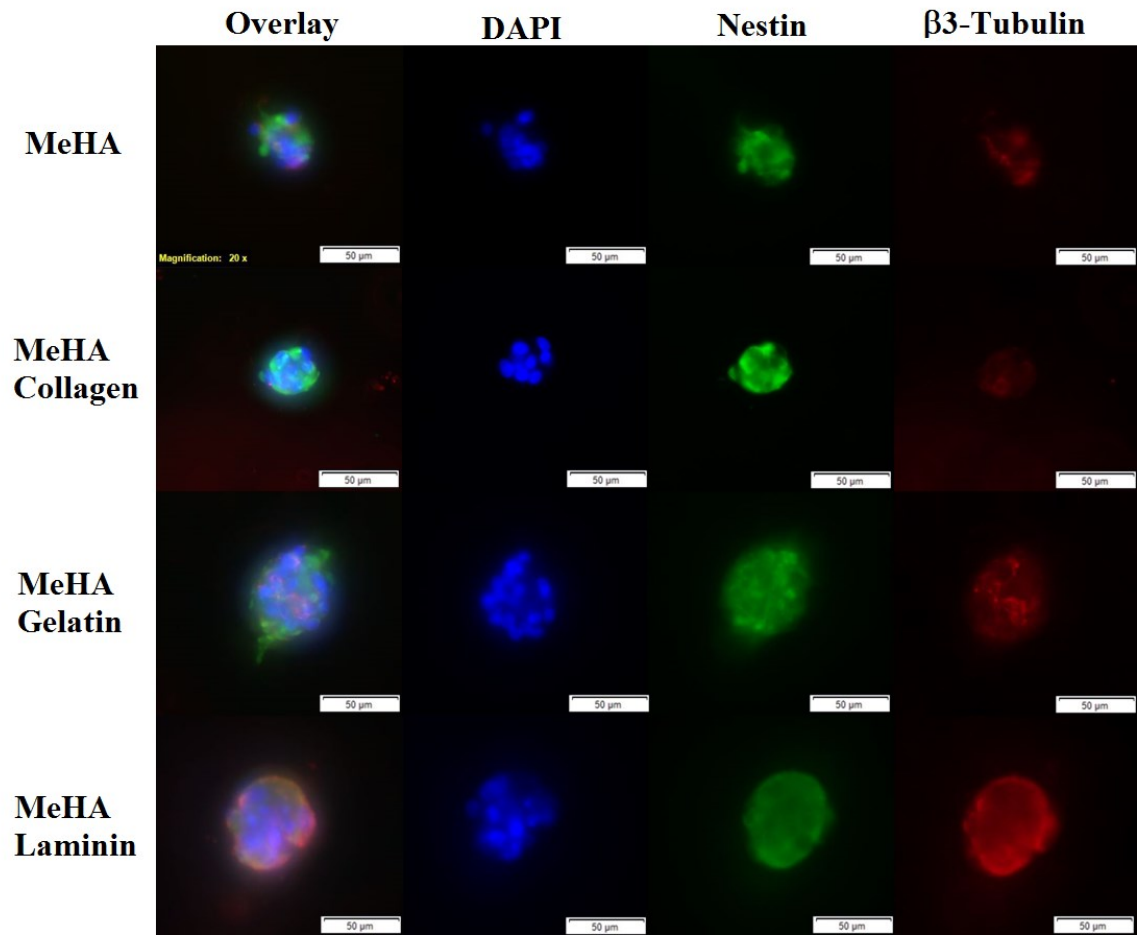

Figure 19. 20x fluorescent microscopy images of RVM encapsulated within hydrogels after 2 weeks of differentiation.

In order to quantify the ICC data, the total percentage of cells expressing nestin and β3-tubulin were calculated by cell counting the number of nuclei and nestin or β3-tubulin in three sections of each well at 20x magnification (Figure 20).

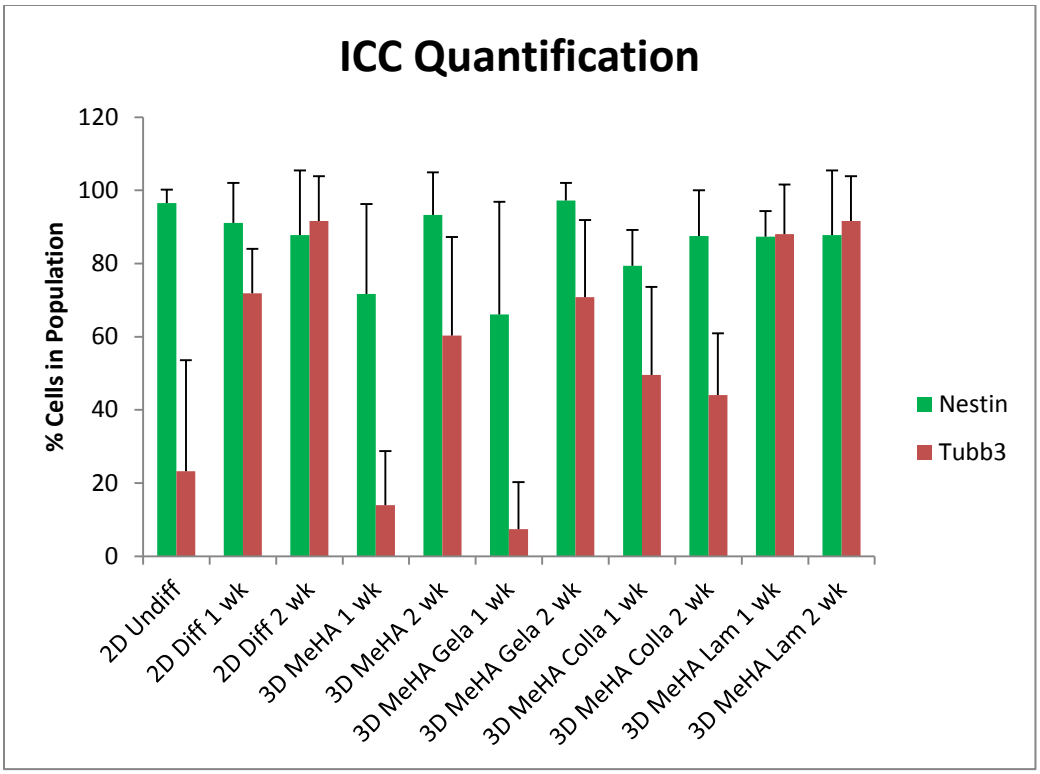

Figure 20. Quantification of cells expressing nestin or β3-tubulin (Tubb3) by cell counting ICC microscopy images at 20x magnification

There also seemed to be a higher cell number in the 2D samples compared to 3D samples. Due to the difficulties in changing medium for the 3D samples, some cells could have been lost over the differentiation process. Furthermore, the working distance on the microscope objectives was insufficient in capturing high resolution images of the neurospheres. The hydrogel samples were 1 mm thick and so were limited to low magnifications. There also seems to be auto-fluorescence coming from certain parts of the hydrogel. In the future, the cell number should be increased and images should be taken on 10x magnification to obtain higher resolution images. Alternatively, a thinner hydrogel may also be used for ICC.

Messenger RNA (mRNA) was collected successfully from both 2D and 3D samples. For the 2D samples, mRNA concentrations between 20 to 40 ng/μL and a 260/280 nm ratio of 1.78 to 2.07 were measured using a plate reader. For all 3D samples

and the 2 week 2D differentiation samples, many of the mRNA concentrations were initially too low (below 15 ng/μL). These samples were concentrated in a vacuum concentrator for 30 minutes. Complementary DNA strands were prepared using a high capacity cDNA prep kit from Applied Biosystems. To match the concentration of cDNA made during RT-PCR between samples, the final concentrations of all samples were normalized to 21.84 ng/μL, which was the lowest concentration measured by the plate reader. After synthesizing cDNA, the cycle threshold (CT) values were measured using a thermal cycler (Eppendorf EP MasterCycler RealPlex) for 40 cycles, using a Taqman RT-qPCR kit from Applied Biosystems. CT values could only be measured from several samples due to low concentrations of mRNA (Table 2 and 3). Asterisks indicate that the CT value measured is from non-triplicate samples.

1 Week Differentiation Average CT Values								
Sample	GAPDH	β-Actin	SOX2	Nestin	β3-tubulin	MAP2	GFAP	OMG
2D MC	20.44	21.05	18.99	20.1	26.5	22.7	17.6	28.97
2D MX	19.46	19.63	18.59	19.66	24.08	21.77	16.74	27.51
MeHA	26.97	31.92	31.83	33.02*	4.09*	-	35.64*	30.27
MeHA-Laminin	20.88*	22.83*	23.48*	23.25*	-	35.47*	21.37*	30.48*
MeHA-Collagen	32.9	34.3*	31.82*	32.14	-	-	33.76	34.56
MeHA-Gelatin	31.56*	34.86*	33.55*	38.83*	-	-	-	33.03*

Table 2. Measured CT values from RT-qPCR for 1 week differentiation samples. CT values denoted with an asterisk indicate sample size of $n < 3$. A dash indicates that CT was not measured within 40 cycles. MC = complete medium change, MX = partial medium exchange (conditioned medium).

2 Week Differentiation Average CT Values								
	GAPDH	β-Actin	SOX2	Nestin	β3-tubulin	MAP2	GFAP	OMG
2D MC	-	-	-	-	-	-	-	-
2D MX	26.46*	29.28*	32.73*	25.23*	-	38.79*	28.93*	34.96*

MeHA	-	-	-	33.21*	-	-	34.57*	-
MeHA-Laminin	26.04*	31.35*	27.69*	23.74*	-	-	24.03*	34.78*
MeHA-Collagen	29.49*	33.68*	31.92*	25.93*	-	-	27.82*	-
MeHA-Gelatin	18.52*	-	-	-	-	-	-	35.61*

Table 3. Measured CT values from RT-qPCR for 2 week differentiation samples. CT values denoted with an asterisk indicate sample size of $n < 3$. A dash indicates that CT was not measured within 40 cycles. MC = complete medium change, MX = partial medium exchange (conditioned medium).

Based on the RT-qPCR results, a comparison of RVM differentiation between 2D and 3D cannot be made. A CT value below 30 should not be analyzed due to the possibility of amplifying human error and non-specific expression. Furthermore, many CT values did not have a sufficient sample number ($n < 3$) to make a statistical comparison. GAPDH and β-Actin is an internal standard that is used to compare expression levels between samples. However, the expression levels of GAPDH and β-Actin had a large deviation in CT value between samples (Figure 21). Therefore, comparisons could not be made using the results from this experiment.

The differentiation experiment will need to be repeated in order to optimize the RT-qPCR collection from 3D hydrogel samples. From these initial results, we have shown that it is possible to retrieve mRNA from cells encapsulated within hydrogels by treating the hydrogels with hyaluronidase. Based on the combined data from ICC and RT-qPCR, it is clear that the MeHA and MeHA with laminin seem to show the best results for neural stem cell differentiation. Further experiments should exclude collagen and gelatin, which is also lacking in the natural brain ECM.

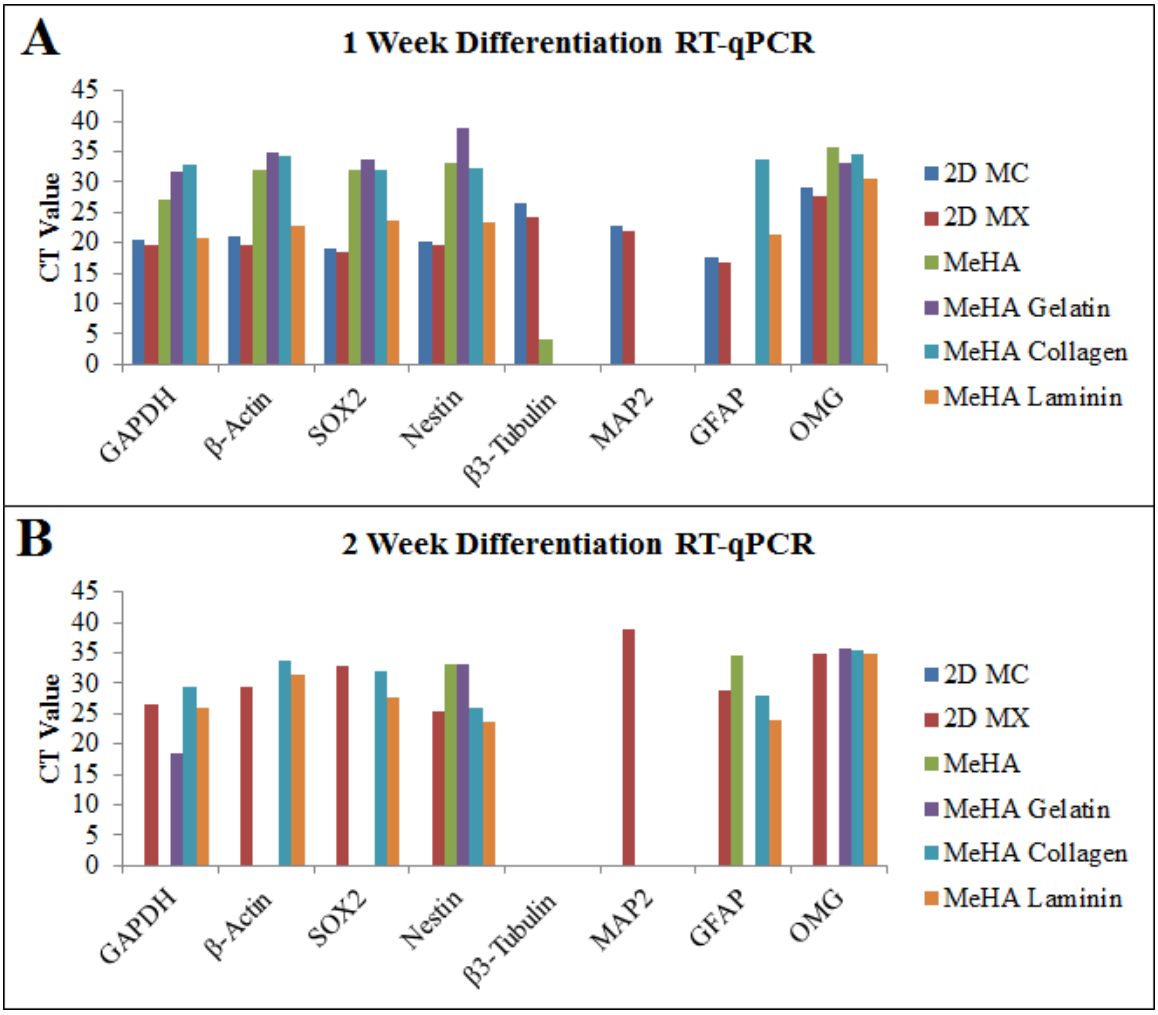

Figure 21. Gene expression level comparisons between samples from RT-qPCR. No standard deviation is shown due to lack of triplicate samples. Samples which took more than 40 cycles are shown as zero.

Further experiments will be necessary to optimize mRNA collection from hydrogel samples. One possibility is to increase the cell number for experiments, or to further concentrate the isolated mRNA prior to RT-qPCR. Furthermore, the MeHA with laminin showed the most consistent results in both ICC and RT-qPCR, indicating its capabilities for neural stem cell studies.

CHAPTER 5: CONCLUSION

In this work, a photo-polymerizable hyaluronic acid hydrogel was characterized by its viscoelastic moduli, swelling ratio, enzymatic degradation, and degree of methacrylation. Additional post-processing by lyophilization yielded a material that could be used for 3D cell culture. The viscoelastic properties of the hydrogel could be matched to adult human brain tissue by modulating its degree of methacrylation, the energy input during crosslinking, and post-processing by lyophilization. The hydrogels had good optical transparency and could be imaged using a microscope with ease.

The effects of the hydrogel on neural stem cell behavior were tested by a 2 week differentiation study. ICC images suggest that the rate of differentiation is similar to cells seeded on laminin coated plastic. However, cells seeded within the hydrogels form neurospheres as opposed to having a more spread morphology. The PCR data was inconclusive, as many of the samples failed to generate CT values below 30 cycles. Furthermore, there was a difference in expression levels of internal standards, GAPDH and β-Actin, between 2D and 3D samples. Further work must be done to optimize the mRNA collection and cDNA amplification process for 3D samples so that accurate comparisons between 2D and 3D differentiations can be made.

REFERENCES

1 Lee, J., Cuddihy, M. J. & Kotov, N. A. Three-dimensional cell culture matrices: state of the art. *Tissue Eng Part B Rev* **14**, 61-86, doi:10.1089/teb.2007.0150 (2008).

2 Roskelley, C. D. & Bissell, M. J. Dynamic reciprocity revisited: a continuous, bidirectional flow of information between cells and the extracellular matrix regulates mammary epithelial cell function. *Biochem Cell Biol* **73**, 391-397 (1995).

3 Nelson, C. M. & Bissell, M. J. Modeling dynamic reciprocity: engineering three-dimensional culture models of breast architecture, function, and neoplastic transformation. *Semin Cancer Biol* **15**, 342-352, doi:10.1016/j.semcancer.2005.05.001 (2005).

4 Lutolf, M. P. & Hubbell, J. A. Synthetic biomaterials as instructive extracellular microenvironments for morphogenesis in tissue engineering. *Nat Biotechnol* **23**, 47-55, doi:10.1038/nbt1055 (2005).

5 Chan, B. P. & Leong, K. W. Scaffolding in tissue engineering: general approaches and tissue-specific considerations. *Eur Spine J* **17 Suppl 4**, 467-479, doi:10.1007/s00586-008-0745-3 (2008).

6 Burdick, J. A. & Vunjak-Novakovic, G. Engineered microenvironments for controlled stem cell differentiation. *Tissue Eng Part A* **15**, 205-219, doi:10.1089/ten.tea.2008.0131 (2009).

7 Griffith, L. G. & Swartz, M. A. Capturing complex 3D tissue physiology in vitro. *Nat Rev Mol Cell Biol* **7**, 211-224, doi:10.1038/nrm1858 (2006).

8 Guilak, F. *et al.* Control of stem cell fate by physical interactions with the extracellular matrix. *Cell Stem Cell* **5**, 17-26, doi:10.1016/j.stem.2009.06.016 (2009).

9 Leipzig, N. D. & Shoichet, M. S. The effect of substrate stiffness on adult neural stem cell behavior. *Biomaterials* **30**, 6867-6878, doi:10.1016/j.biomaterials.2009.09.002 (2009).

10 Saha, K. *et al.* Substrate modulus directs neural stem cell behavior. *Biophys J* **95**, 4426-4438, doi:10.1529/biophysj.108.132217 (2008).

11 Hoffman, A. Hydrogels for biomedical applications. *Advanced Drug Delivery Reviews* **54**, 3-12, doi:10.1016/S0169-409X(01)00239-3 (2002).

12 Cui, F., Tian, W., Hou, S., Xu, Q. & Lee, I. Hyaluronic acid hydrogel immobilized with RGD peptides for brain tissue engineering. *Journal of*

Materials Science-Materials in Medicine **17**, 1393-1401, doi:10.1007/s10856-006-0615-7 (2006).

13 Park, Y. D., Tirelli, N. & Hubbell, J. A. Photopolymerized hyaluronic acid-based hydrogels and interpenetrating networks. *Biomaterials* **24**, 893-900 (2003).

14 Jeon, O. *et al.* Mechanical properties and degradation behaviors of hyaluronic acid hydrogels cross-linked at various cross-linking densities. *Carbohydrate Polymers* **70**, 251-257, doi:10.1016/j.carbpol.2007.04.002 (2007).

15 Drury, J. L. & Mooney, D. J. Hydrogels for tissue engineering: scaffold design variables and applications. *Biomaterials* **24**, 4337-4351 (2003).

16 Takeshita, Y. *et al.* An in vitro blood-brain barrier model combining shear stress and endothelial cell/astrocyte co-culture. *J Neurosci Methods* **232**, 165-172, doi:10.1016/j.jneumeth.2014.05.013 (2014).

17 Ruoslahti, E. Brain extracellular matrix. *Glycobiology* **6**, 489-492, doi:10.1093/glycob/6.5.489 (1996).

18 Wang, D. & Fawcett, J. The perineuronal net and the control of CNS plasticity. *Cell Tissue Res* **349**, 147-160, doi:10.1007/s00441-012-1375-y (2012).

19 McRae, P. A. & Porter, B. E. The perineuronal net component of the extracellular matrix in plasticity and epilepsy. *Neurochem Int* **61**, 963-972, doi:10.1016/j.neuint.2012.08.007 (2012).

20 Burdick, J., Chung, C., Jia, X., Randolph, M. & Langer, R. Controlled degradation and mechanical behavior of photopolymerized hyaluronic acid networks. *Biomacromolecules* **6**, 386-391, doi:10.1021/bm049508a (2005).

21 Kim, J. *et al.* Bone regeneration using hyaluronic acid-based hydrogel with bone morphogenic protein-2 and human mesenchymal stem cells. *Biomaterials* **28**, 1830-1837, doi:10.1016/j.biomaterials.2006.11.050 (2007).

22 Burdick, J. & Prestwich, G. Hyaluronic Acid Hydrogels for Biomedical Applications. *Advanced Materials* **23**, H41-H56, doi:10.1002/adma.201003963 (2011).

23 Kogan, G., Soltes, L., Stern, R. & Gemeiner, P. Hyaluronic acid: a natural biopolymer with a broad range of biomedical and industrial applications. *Biotechnology Letters* **29**, 17-25, doi:10.1007/s10529-006-9219-z (2007).

24 Ibrahim, S., Kothapalli, C. R., Kang, Q. K. & Ramamurthi, A. Characterization of glycidyl methacrylate - crosslinked hyaluronan hydrogel scaffolds incorporating elastogenic hyaluronan oligomers. *Acta Biomater* **7**, 653-665, doi:10.1016/j.actbio.2010.08.006 (2011).

25 Sabnis, A., Rahimi, M., Chapman, C. & Nguyen, K. T. Cytocompatibility studies of an in situ photopolymerized thermoresponsive hydrogel nanoparticle system using human aortic smooth muscle cells. *J Biomed Mater Res A* **91**, 52-59, doi:10.1002/jbm.a.32194 (2009).

26 Lledo, P. M., Alonso, M. & Grubb, M. S. Adult neurogenesis and functional plasticity in neuronal circuits. *Nat Rev Neurosci* **7**, 179-193, doi:10.1038/nrn1867 (2006).

27 Kim, S. U., Lee, H. J. & Kim, Y. B. Neural stem cell-based treatment for neurodegenerative diseases. *Neuropathology* **33**, 491-504, doi:10.1111/neup.12020 (2013).

28 Chuang, J. H., Tung, L. C. & Lin, Y. Neural differentiation from embryonic stem cells in vitro: An overview of the signaling pathways. *World J Stem Cells* **7**, 437-447, doi:10.4252/wjsc.v7.i2.437 (2015).

29 Okolicsanyi, R. K., Griffiths, L. R. & Haupt, L. M. Mesenchymal stem cells, neural lineage potential, heparan sulfate proteoglycans and the matrix. *Dev Biol* **388**, 1-10, doi:10.1016/j.ydbio.2014.01.024 (2014).

30 Salimi, A., Nadri, S., Ghollasi, M., Khajeh, K. & Soleimani, M. Comparison of different protocols for neural differentiation of human induced pluripotent stem cells. *Mol Biol Rep* **41**, 1713-1721, doi:10.1007/s11033-014-3020-1 (2014).

31 Chen, B. Y. *et al.* Brain-derived neurotrophic factor stimulates proliferation and differentiation of neural stem cells, possibly by triggering the Wnt/β-catenin signaling pathway. *J Neurosci Res* **91**, 30-41, doi:10.1002/jnr.23138 (2013).

32 Liu, F. *et al.* Combined effect of nerve growth factor and brain‐derived neurotrophic factor on neuronal differentiation of neural stem cells and the potential molecular mechanisms. *Mol Med Rep* **10**, 1739-1745, doi:10.3892/mmr.2014.2393 (2014).

33 Cattaneo, E. & McKay, R. Proliferation and differentiation of neuronal stem cells regulated by nerve growth factor. *Nature* **347**, 762-765, doi:10.1038/347762a0 (1990).

34 Yi, X., Jin, G., Tian, M., Mao, W. & Qin, J. Porous chitosan scaffold and ngf promote neuronal differentiation of neural stem cells in vitro. *Neuro Endocrinol Lett* **32**, 705-710 (2011).

35 Tonge, P. D. & Andrews, P. W. Retinoic acid directs neuronal differentiation of human pluripotent stem cell lines in a non-cell-autonomous manner. *Differentiation* **80**, 20-30, doi:10.1016/j.diff.2010.04.001 (2010).

36 Okada, Y., Shimazaki, T., Sobue, G. & Okano, H. Retinoic-acid-concentration-dependent acquisition of neural cell identity during in vitro differentiation of

mouse embryonic stem cells. *Dev Biol* **275**, 124-142, doi:10.1016/j.ydbio.2004.07.038 (2004).

37 Su, H. *et al.* Lithium enhances the neuronal differentiation of neural progenitor cells in vitro and after transplantation into the avulsed ventral horn of adult rats through the secretion of brain-derived neurotrophic factor. *J Neurochem* **108**, 1385-1398, doi:10.1111/j.1471-4159.2009.05902.x (2009).

38 Vazey, E. M. & Connor, B. Differential fate and functional outcome of lithium chloride primed adult neural progenitor cell transplants in a rat model of Huntington disease. *Stem Cell Res Ther* **1**, 41, doi:10.1186/scrt41 (2010).

39 Previtera, M. L. *et al.* The effects of substrate elastic modulus on neural precursor cell behavior. *Ann Biomed Eng* **41**, 1193-1207, doi:10.1007/s10439-013-0765-y (2013).

40 Seidlits, S. *et al.* The effects of hyaluronic acid hydrogels with tunable mechanical properties on neural progenitor cell differentiation. *Biomaterials* **31**, 3930-3940, doi:10.1016/j.biomaterials.2010.01.125 (2010).

41 Huang, Y. J., Wu, H. C., Tai, N. H. & Wang, T. W. Carbon nanotube rope with electrical stimulation promotes the differentiation and maturity of neural stem cells. *Small* **8**, 2869-2877, doi:10.1002/smll.201200715 (2012).

42 Kobelt, L. J., Wilkinson, A. E., McCormick, A. M., Willits, R. K. & Leipzig, N. D. Short duration electrical stimulation to enhance neurite outgrowth and maturation of adult neural stem progenitor cells. *Ann Biomed Eng* **42**, 2164-2176, doi:10.1007/s10439-014-1058-9 (2014).

43 Pires, F., Ferreira, Q., Rodrigues, C. A., Morgado, J. & Ferreira, F. C. Neural stem cell differentiation by electrical stimulation using a cross-linked PEDOT substrate: Expanding the use of biocompatible conjugated conductive polymers for neural tissue engineering. *Biochim Biophys Acta* **1850**, 1158-1168, doi:10.1016/j.bbagen.2015.01.020 (2015).

44 Itoh, T., Satou, T., Dote, K., Hashimoto, S. & Ito, H. Effect of basic fibroblast growth factor on cultured rat neural stem cell in three-dimensional collagen gel. *Neurol Res* **27**, 429-432, doi:10.1179/016164105X18476 (2005).

45 Green, M. A., Bilston, L. E. & Sinkus, R. In vivo brain viscoelastic properties measured by magnetic resonance elastography. *NMR Biomed* **21**, 755-764, doi:10.1002/nbm.1254 (2008).

46 Williams, C. G., Malik, A. N., Kim, T. K., Manson, P. N. & Elisseeff, J. H. Variable cytocompatibility of six cell lines with photoinitiators used for polymerizing hydrogels and cell encapsulation. *Biomaterials* **26**, 1211-1218, doi:10.1016/j.biomaterials.2004.04.024 (2005).

47 Bahney, C. *et al.* Visible Light Photoinitiation of Mesenchymal Stem Cell-Laden Bioresponsive Hyrogels. *European Cells & Materials* **22**, 43-55 (2011).

48 Bryant, S., Nuttelman, C. & Anseth, K. Cytocompatibility of UV and visible light photoinitiating systems on cultured NIH/3T3 fibroblasts in vitro. *Journal of Biomaterials Science-Polymer Edition* **11**, 439-457, doi:10.1163/156856200743805 (2000).

49 Preston, M. & Sherman, L. S. Neural Stem Cell Niches: Critical Roles for the Hyaluronan-Based Extracellular Matrix in Neural Stem Cell Proliferation and Differentiation. *Front Biosci* **3**, 1165 - 1179 (2011).